ACS APPLIED MATERIALS & INTERFACES

Research Article

www.acsami.org

Surface Engineering of Graphene Quantum Dots and Their Applications as Efficient Surfactants

Han-Hee Cho, Hyunseung Yang, Dong Jin Kang, and Bumjoon J. Kim*

Department of Chemical and Biomolecular Engineering, Korea Advanced Institute of Science and Technology (KAIST), Daejeon 305−701, Korea

Supporting Information

ABSTRACT: The surface properties of graphene quantum dots (GQDs) control their dispersion and location within the matrices of organic molecules and polymers, thereby determining various properties of the hybrid materials. Herein, we developed a facile, one-step method for achieving systematic control of the surface properties of highly fluorescent GQDs. The surfaces of the as-synthesized hydrophilic GQDs were modified precisely depending on the number of grafted hydrophobic hexylamine. The geometry of the modified GQDs was envisioned by conducting simulations using density functional theory. In stark contrast to the pristine GQDs, the surface-modified GQDs can effectively stabilize oil-in-water Pickering emulsions and submicron-sized colloidal particles in mini-emulsion polymerization. These versatile GQD surfactants were also employed in liquid−solid systems; we demonstrated their use for tailoring the dispersion of graphite in methanol. Finally, the particles produced by the GQD surfactants were fluorescent due to luminescence of the GQDs, which offers great potential for various applications, including fluorescent sensors and imaging.

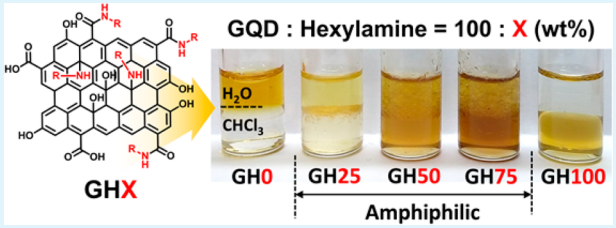

KEYWORDS: *graphene quantum dots, surface modification, surfactants, Pickering emulsion, amphiphilicity*

INTRODUCTION

Nanoparticles (NPs) with tailored surface properties can control the interfacial properties of two immiscible polymers or fluids; thus, they can act as efficient surfactants to produce novel structured materials such as bicontinuous solar cells, membranes for catalytic supports, photonic band gap materials, and asymmetric-structured particles.[1−15] Unlike conventional organic surfactants, NP surfactants have the interesting photonic, magnetic, electrical, and catalytic properties that can be combined to produce synergistic effects with the intrinsic properties of the polymer or fluid matrix. In addition, extremely stable emulsions can be easily developed by particle surfactants due to their quasi-irreversible adsorption at the interface between the blends.[16−21] However, the efficiencies of the NP surfactants are often limited due to their ill-defined surface properties, which determine their dispersion and control their thermodynamic interactions with the matrix materials.[17,22−25] Therefore, an appropriate method must be developed to precisely tune the surface properties of the NPs. However, this remains a significant challenge, because each type of NPs has a unique surface coating, which often requires different strategies for tailoring their surface chemistry.[26]

Nanometer-sized graphite derivatives called graphene quantum dots (GQDs) have been the center of intensive research due to their remarkable physical, mechanical, and optoelectronic properties.[27−34] They consist of hydrophilic groups at the edge and a hydrophobic basal plane similar to well-known graphene oxide (GO), but they have a greater edge-to-volume ratio than micron-sized GO.[4,35,36] Therefore, GQDs have great potential for use as effective surfactants that are suitable for the development of the submicron-sized emulsions or colloidal particles. In addition, their distinctive properties, such as tunable luminescence emissions, biocompatibility, and long-term resistance to photobleaching, make promising applications of GQD-stabilized emulsions feasible, such as their use in bioimaging and fluorescent sensors.[27−33,37−40] However, GQDs have seldom been used as solid surfactants, because it is difficult to control their surface properties in a reproducible and systematic manner.[41] Unlike GO sheets, the surfaces of GQDs are highly hydrophilic due to the excessive numbers of oxygen functional groups on the basal plane and edges, which limits their solubility in the organic solvents.[4,35,36,42,43] Recently, it was reported that the surface of the GQDs could be modified by the chemical-grafting approach.[37−39] Nevertheless, chemically modified GQDs have yet to be used as surfactants because the precise and systematic control in the surface properties of GQDs by chemical-grafting approach has not been achieved.

Herein, we report a simple, one-step method to produce nano-sized GQDs with controlled surface activity (Scheme 1). As-synthesized hydrophilic GQDs were modified with hydrophobic hexylamine via one-step simultaneous reaction of *N*,*N*′-dicyclohexylcarbodiimide (DCC) coupling and epoxide ring-opening at a mild temperature of 40 °C. Specifically, we

Received: January 23, 2015
Accepted: March 31, 2015
Published: March 31, 2015

DOI: 10.1021/acsami.5b00729
ACS Appl. Mater. Interfaces 2015, 7, 8615−8621

Scheme 1. Preparation Route of Surface-Modified GQDs with Hexylamines[a]

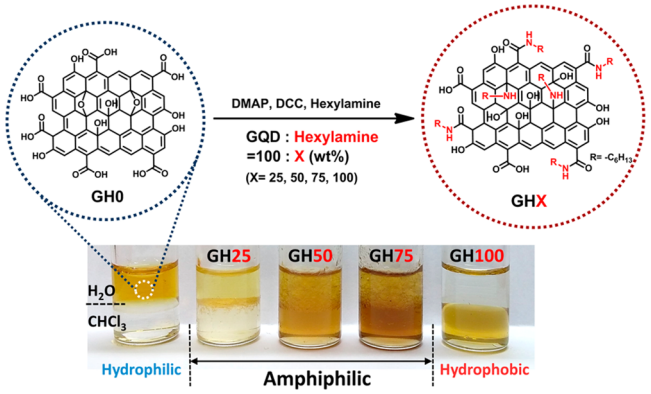

[a]Photo images describe the solubilities of the GQDs.

developed a series of four different modified GQDs that had gradually increasing amounts of grafted hexylamine, and we demonstrated a full-range control of the surface properties of the GQDs, i.e., from very hydrophilic to fully hydrophobic. Based on the controlled hydrophilic/hydrophobic balance of the modified GQDs, their effectiveness as particle surfactants was examined in various immiscible blends. In addition, all of the emulsions and particles stabilized by the GQD surfactants were highly stable and fluorescent, demonstrating a successful example of the synergistic incorporation of the unique GQD properties into the composites.

EXPERIMENTAL SECTION

Materials. Vulcan CX-72 carbon black was purchased from Cabot Corporation. Styrene, hexylamine, DCC, 4-dimethylaminopyridine (DMAP), and toluene were purchased from Aldrich. Before the emulsion polymerization, styrene was purified by passing it through an alumina column. Azobis(isobutyronitrile) (AIBN) was purchased from Junsei and purified by recrystallization from ethanol. Deionized water was used in all of the experiments.

Preparation of Pristine GQDs and Surface Modified GQDs. Pristine GQDs were prepared via chemical oxidation.[44] Briefly, CX-72 carbon black was refluxed with nitric acid (6 M) for 48 h. Then, the resulting mixture was cooled to room temperature and centrifuged at 4000 rpm for 20 min. The supernatant was carefully collected, and a reddish-brown powder was obtained by evaporating the solvent. The GQDs were redispersed in tetrahydrofuran (THF) and ultrafiltered through a 0.22 μm microporous membrane. To prepare the surface-modified GQDs, hexylamine (25 mg, 0.247 mmol), DMAP (60.3 mg, 0.494 mmol), and the as-prepared GQDs (100 mg) were dissolved in THF (20 mL) with nitrogen bubbling, and the mixture was stirred for 30 min. Then, DCC (203.3 mg, 0.988 mmol) was added, and the mixture was heated at 40 °C for 12 h. After cooling to room temperature, the mixture was passed through Whatman #1 filter paper. The filtrate was centrifuged, and the precipitated product was then washed with diethyl ether several times to remove unreacted hexylamine. The product was named **GH25**. Similar procedures were used to synthesize **GH50**, **GH75**, and **GH100** with different weight ratios of hexylamine to pristine GQDs, i.e., 50, 75, and 100 wt %, respectively.

Preparation of Pickering Emulsions Stabilized by Modified GQDs. Solutions of modified GQDs were prepared by dissolving **GH0** and **GH25** (3 mg) in deionized (DI) water (2 mL) and **GH50**, **GH75**, and **GH100** in 1 mL of *o*-dichlorobenzene (DCB) and subsequently subjecting them to ultrasonication for 10 min. Then, 1 mL of DCB was added to the **GH0** and **GH25** solutions, and 2 mL of water were added to **GH50**, **GH75**, and **GH100** to prepare the same overall amount of solution (3 mL) for each sample. The solutions were emulsified using a homogenizer for 5 min at 15 000 rpm.

Preparation of Polystyrene (PS) Colloidal Particles. PS colloidal particles were prepared by heterogeneous mini-emulsion polymerization. In a 50 mL vial, GQDs (7.5 mg), styrene (100 mg), octadecane (5 mg), and AIBN (4 mg) were dispersed in methanol (MeOH) and stirred for 20 min. The mixture was subsequently subjected to ultrasonication for 10 min. The resulting mixture was transferred to an ampule and then degassed three times before performing the radical reaction. The reaction mixture was stirred at a constant rate at 70 °C for 24 h. After polymerization, the PS colloidal particles were quenched by pouring the reaction mixture into MeOH at room temperature. The PS colloidal particles were isolated by filtration and washed several times with MeOH, a MeOH/distilled water (50:50 v/v) mixture, and distilled water and finally dried at room temperature.

Dispersion of Graphite. For the solid dispersion experiments, graphite powder (Asbury, 3763) and 3 mg of GQDs were added to 3 mL of MeOH at a mass ratio of 5:1 (graphite/GQD). Then, the dispersion was sonicated for 30 min using an ultrasonicator. After that, the solution was centrifuged at 1000 rpm for 5 min to remove undispersed chunks. The supernatant was carefully collected and stored at room temperature for several months. Then, images of the dispersed graphite were obtained by optical microscopy.

Characterization. The size of GQDs and the morphology of polymer particles stabilized by modified GQDs were investigated using field emission-scanning electron microscope (FE-SEM; Hitachi S-4800), transmission electron microscopy (TEM; JEOL 2000FX), and optical microscopy (Nikon, Eclipse 80i). The TEM samples were prepared by dropping aqueous suspensions of GQDs on Cu grids coated with a holey carbon film followed by solvent evaporation. Attenuated total reflectance-Fourier transform infrared (ATR-FTIR) spectra were collected using a Bruker ALPHA. X-ray photoelectron spectroscopy (XPS) was performed using a Thermo VG Scientific ESCA 2000. Atomic force microscopy (AFM) images were acquired on a scanning probe microscope (Veeco). X-ray diffraction (XRD) was performed using a RIGAKU D/MAX-2500. Raman spectra were collected using a LabRAM ARAMIS. The UV−vis absorption spectra and photoluminescence (PL) emission spectra of the surface-modified GQDs were measured using a UV-1800 spectrophotometer (Shimadzu Scientific Instruments) and a Horiba Jovin Yvon NanoLog spectrophotometer, respectively. The emission quantum yields (QYs) of the surface-modified GQDs were calculated based on rhodamine B as a standard using the following equation:

$$\Phi_x = \Phi_{st}\frac{I_x}{I_{st}}\frac{\eta_x^2}{\eta_{st}^2}\frac{A_{st}}{A_x}$$

where Φ is the quantum yield, I is the measured integrated emission intensity, η is the refractive index of the solvent, A is the optical density, and the subscript "st" refers to the standard with a known quantum yield, and "x" refers to the sample.

RESULTS AND DISCUSSION

The pristine GQDs were synthesized according to the reported procedure and denoted as **GH0**.[44] The resulting **GH0** exhibited a broad (002) XRD peak centered at 21.1°, which was similar to the value from hydrothermally synthesized GQDs (**Figure S1(a)**, Supporting Information).[44] In addition, upon the excitation of the **GH0** with a 514 nm laser, the Raman spectrum showed two distinctive carbon-related bands, D band at around 1356 cm^{-1} and G band at around 1605 cm^{-1}, which was consistent with previous reports (Figure S1(b)).[28,38,40] The **GH0** had various oxygen-containing groups, such as epoxy, hydroxyl, and carboxylic acid groups on the basal plane and the edges. These functional groups can provide reactive sites for interactions with organic molecules. Scheme 1 shows that the surface chemistry of the GQDs was systematically modified by

DOI: 10.1021/acsami.5b00729
ACS Appl. Mater. Interfaces 2015, 7, 8615−8621

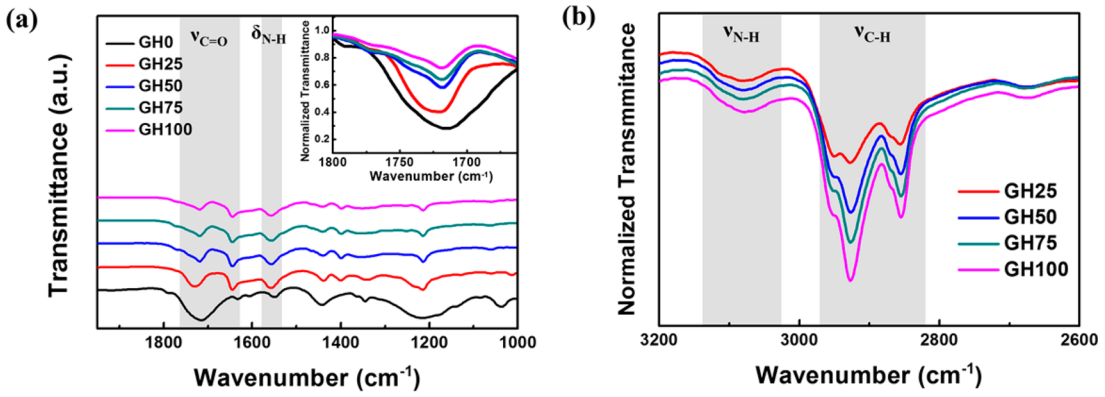

Figure 1. (a) Transmission infrared spectra of **GH0**, **GH25**, **GH50**, **GH75**, and **GH100** (inset: vector-normalized transmission infrared spectra for a specified peak of the carboxyl group around 1720 cm^{-1}); (b) vector-normalized transmission infrared spectra of **GH25**, **GH50**, **GH75**, and **GH100** ranging from 3200 to 2600 cm^{-1}.

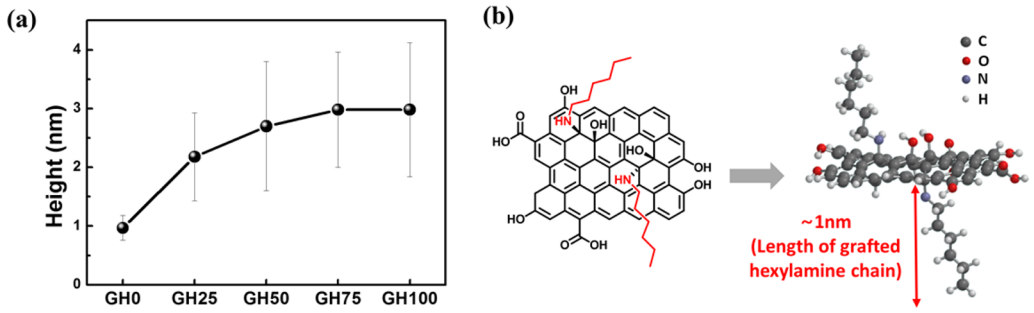

Figure 2. (a) Average height of the synthesized GQDs measured by AFM; (b) chemical structure of model GQD system with two grafted hexylamine on the basal plane and its equilibrium geometry based on molecular simulations.

altering the amounts of hexylamine molecules. These molecules were grafted onto the GQD surface by one-step reaction of DCC coupling with the carboxylic acid moieties and/or of the ring-opening of the epoxy moieties at a mild temperature of 40 °C. As a result, four different types of GQDs were obtained successfully, and they are denoted as **GH25**, **GH50**, **GH75**, and **GH100** according to their weight ratios of added hexylamines, i.e., 25, 50, 75, and 100 wt %, respectively.

ATR-FTIR measurements were performed to monitor the grafting reaction of the hexylamine occurred on the surfaces of the GQDs (Figure 1). A few important vibration peaks of functional groups were monitored and compared, including carboxylic acid, epoxide, and amide groups. For **GH0**, a strong stretching vibration of C═O was observed at 1720 cm^{-1} due to the carboxylic acid groups at the GQD edges. However, the intensity of the C═O stretching vibrations decreased gradually in the order of **GH25**, **GH50**, **GH75**, and **GH100** (inset in Figure 1a), because the carboxylic acid groups were converted to amide groups, resulting in the appearance of new stretching vibration of C═O at 1644 cm^{-1} and of bending vibration of N−H at 1557 cm^{-1}. Also, the stretching vibrations of secondary amine appeared at 3050−3150 cm^{-1}, whereas the epoxide band at 1035 cm^{-1} decreased in intensity due to the ring-opening reaction of epoxide groups with the hexylamine. In addition, asymmetric stretching vibration peaks of C−H at 2854 and 2927 cm^{-1} increased as the amount of grafted hexylamine increased in the order of **GH25**, **GH50**, **GH75**, and **GH100**. For further support of the precise surface modification of the GQDs, high-resolution carbon 1s (C 1s) and nitrogen 1s (N 1s) XPS measurements were performed (Figure S2). Table S1 summarizes the atomic concentrations of the different GQDs measured by XPS. The variations between the **GH0** and **GH100** C 1s spectra revealed significant changes in the proportions of carboxylic acid and amide groups. For **GH100**, because most of the carboxylic acid groups reacted with the hexylamine, the C(O)−O peak at 289.4 eV vanished, whereas an amide bond (C(O)−N) peak appeared at 288.1 eV. In the N 1s XPS spectra, it was evident that the total amount of nitrogen increased in order of **GH0**, **GH25**, **GH50**, **GH75**, and **GH100**, indicating that the GQD surface properties were systematically controlled by the successful grafting of hexylamine molecules onto the GQDs.

The average heights of the surface-modified GQDs were measured from the AFM images, and their average sizes were estimated from the TEM images of each sample. As shown in Figure S3, **GH0** was monodispersed with an average height of 0.97 nm, indicating that it was mostly single- or bilayered.[45] Interestingly, upon the grafting of the hexylamine, the average height of **GH100** was increased dramatically to 2.98 nm, with clear increasing trend in the order of **GH25**, **GH50**, **GH75**, and **GH100** (Figure 2a). The increase in the average height was attributed to the chain length of the hexylamine grafted on the basal plane of the GQDs, which can be well supported by molecular simulation.[37] The simulation was performed using density functional theory (DFT) at the B3LYP/6-31G(d,p) level based on the GQD model that had two hexylamine grafted on the basal plane (Figure 2b). Since the chain length of the extended hexylamine molecule was about 1 nm at the equilibrium geometry, the calculated height of the hexylamine-grafted GQDs was approximately 3 nm, which was consistent with our experimental results. In addition, the grafting of hexylamine affected the size of the GQDs. As shown in Figure

DOI: 10.1021/acsami.5b00729
ACS Appl. Mater. Interfaces 2015, 7, 8615−8621

S4, the size increased from 12.4 for **GH0** to 13.5 nm for **GH100**, validating that the hexylamine molecules were successfully grafted onto the GQD edges. And, as shown in insets of Figure S4(a) and (d), the high-resolution TEM images of **GH0** and **GH75** revealed a crystalline structure with a lattice parameter of 0.24 nm, which corresponds to the (1120) lattice fringes of graphene, suggesting that the crystalline structures of the GQDs were maintained after the hexylamine grafting.[40]

To investigate the effect of the modified surface chemistry on the solubility of the GQDs, 3 mg of each type of the five different GQDs were separately dissolved in 2 mL of a water/chloroform (1:1 v/v) mixture (Figure S6). Whereas **GH0** was only soluble in the water phase, most of **GH25**, **GH50**, and **GH75** were located at the interface between the water and the organic phase. In contrast, **GH100** was soluble only in the organic phase. Thus, the surface properties of the modified GQDs were controlled systematically, ranging from hydrophilic to hydrophobic surfaces. Furthermore, to demonstrate the solubility of the surface-modified GQDs, **GH25**, **GH50**, **GH75**, and **GH100** were dispersed in other hydrophobic solvents, such as dichloromethane (DCM), toluene, chlorobenzene (CB), and DCB. As shown in Figure S7, the **GH50**, **GH75**, and **GH100** were clearly dispersed in these solvents without any aggregation. However, the **GH25** was only partially dispersed due to relatively strong hydrophilic surface properties. Next, we explored the potential of the surface-modified GQDs for use as surfactants to create micrometer-sized droplets of organic solvent in water. For each of the five different GQDs, a 1 mg·mL^{-1} GQD solution in a DCB/water (1:2 v/v) mixture was emulsified using a homogenizer at 15 000 rpm for 5 min to generate an oil-in-water emulsion. Even after vigorous stirring, **GH0** and **GH100** remained in a single phase, i.e., water and DCB, respectively; thus, they failed to form Pickering emulsions. In contrast, as shown in Figure 3b–d, **GH25**, **GH50**, and **GH75** reduced the total interfacial energy by replacing part of the oil–water at the interface, resulting in the dispersion of the oil droplets in the water.[1,2,46–48] The optical microscopy images were obtained three months after preparation of the emulsions. Most of the emulsified droplets were approximately 2–3 μm in diameter, demonstrating the high interfacial activity of **GH25**, **GH50**, and **GH75**. However, each sample had a different volume fraction of the residual emulsion; 9, 77, and 76 vol % for **GH25**, **GH50**, and **GH75**, respectively (Figure 3a).[49] In addition, the **GH50** and **GH75** emulsions were stable against coalescence for at least several months, because the grafted hexylamines on the GQDs suppressed the aggregation of the GQDs significantly by reducing the strong $\pi-\pi$ interactions between the GQDs.

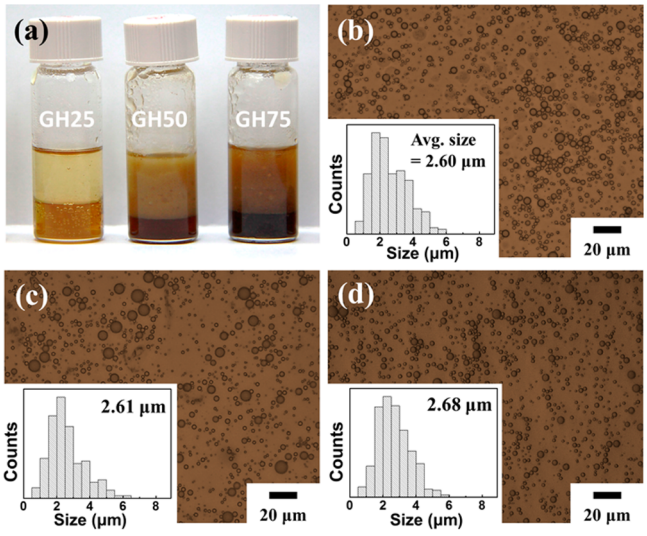

Figure 3. (a) Photograph of the Pickering emulsions stabilized by **GH25**, **GH50**, and **GH75**. Optical micrographs of DCB-in-water Pickering emulsions stabilized by (b) **GH25**, (c) **GH50**, and (d) **GH75**. **GH0** and **GH100** were not able to stabilize the Pickering emulsions. The insets in panels b–d show the size distributions and average sizes of the emulsion droplets.

The amphiphilic nature of **GH25**, **GH50**, and **GH75** allowed for their use as surfactants in heterogeneous polymerization. Mini-emulsion polymerization of styrene was performed at 70 °C for 24 h using the GQDs as surfactants. PS colloidal particles were not produced when **GH0** and **GH100** were employed, which is consistent with the results from the Pickering emulsions. In contrast, the mini-emulsion polymerization using **GH25**, **GH50**, and **GH75** produced submicron-sized and spherical PS colloidal particles with smooth surfaces that resembled the surface morphology of particles stabilized by conventional organic surfactants (Figure 4). These surface morphologies differ from the rough surface morphologies observed for the PS colloidal particles formed when large GO sheets were used as the stabilizers.[50,51] The conversions of all mini-emulsion polymerizations were greater than 90%, substantiating the effectiveness of the surfactant behaviors of **GH25**, **GH50**, and **GH75**. The average sizes of the PS colloidal particles stabilized by **GH25**, **GH50**, and **GH75** were 655, 641, and 278 nm, respectively. In addition, the particle size distributions became narrower in the order of **GH25**, **GH50**, and **GH75**, indicating that **GH75** had the highest interfacial activity of the GQDs used in this study due to its well-balanced amphiphilicity. Furthermore, the tunable luminescence emission of the GQDs can be synergistically combined with surfactant properties. We measured the UV–vis absorption spectra and photoluminescence (PL) emission spectra of **GH25**, **GH50**, and **GH75** to investigate the luminescence properties of the GQDs. As shown in Figure S8(a), strong absorption bands for the surface-modified GQDs were observed at around 278 nm, which was attributed to amide groups at the edges of the GQDs.[52] Figure S8(b) shows PL emission spectra of **GH25**, **GH50**, and **GH75** under excitation at 365 nm. All of the surface-modified GQDs emitted green luminescence with maximum emission peaks at 540 nm, irrespective of the amount of grafted hexylamine. It is suggested that PL emission of GQDs results from the irradiation decay of excited electrons from the lowest unoccupied molecular orbital (LUMO) to highest occupied molecular orbital (HOMO) of the carbenes at their zigzag edges.[37,38,40] In addition, the carbenes at the zigzag edges of the pristine GQDs were expected to be well preserved even after hexylamine chains were grafted onto the edges of the GQDs because those sites were not affected by the surface modifications. Therefore, PL emissions were well observed for the surface-modified GQDs, i.e., **GH25**, **GH50**, and **GH75**. The QYs of the surface-modified GQDs were calculated based on rhodamine B as a standard. The QYs of **GH25**, **GH50**, and **GH75** decreased slightly in the order of 1.91, 1.56, and 1.41%, respectively. The –CONHR and –CNHR groups formed by the surface modification induced the nonradiative recombination of localized electron–hole pairs; thus, the QY decreased gradually as the amount of grafted hexylamine increased.[37] To

DOI: 10.1021/acsami.5b00729
ACS Appl. Mater. Interfaces 2015, 7, 8615–8621

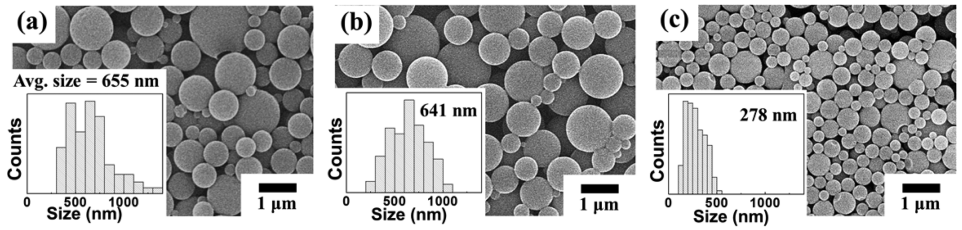

Figure 4. SEM images and the size distributions of the PS colloidal particles prepared by mini-emulsion polymerization using (a) **GH25**, (b) **GH50**, and (c) **GH75**. The insets in panels a–c show the size distributions and average sizes of the PS colloidal particles.

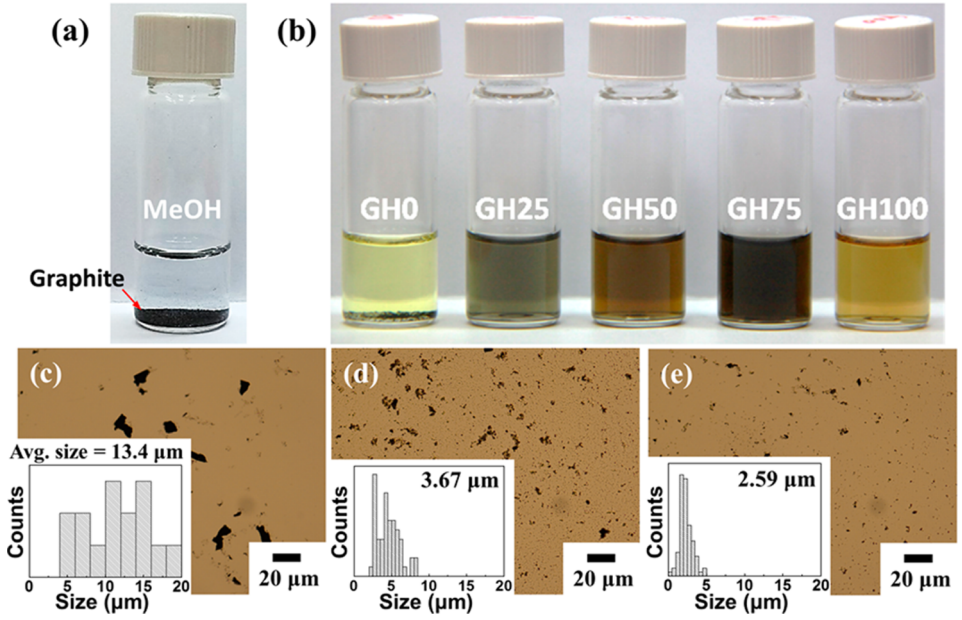

Figure 5. Photographs of graphite powder in MeOH (a) without a dispersing agent and (b) with **GH0**, **GH25**, **GH50**, **GH75**, and **GH100** as dispersing agents after several months. Optical microscopy images and size distribution histograms of the graphite dispersions using (c) **GH25**, (d) **GH50**, and (e) **GH75**.

demonstrate potential of the surface-modified GQDs as fluorescent surfactants, the optical and fluorescence microscopy images of PS particles stabilized by **GH25** were measured. Figure S9 shows that the PS colloidal particles stabilized by **GH25** had a green emission, which indicated that fluorescent GQDs were strongly coated on the surface of the PS particles.

Another major application of surfactants is as dispersing agents for insoluble solids by reducing the interfacial energy between the solid and the liquid.[4] To investigate the surfactant behaviors of surface modified GQDs for solid dispersions, a model system with graphite as the insoluble solid and MeOH as the solvent was chosen (Figure 5a). The graphite powder and GQDs were dispersed in MeOH at a mass ratio of 5:1, and the dispersion was sonicated for 30 min using an ultrasonicator. Then, the dispersion was centrifuged at 1000 rpm for 5 min for separation. Because the GQDs have π-conjugated aromatic rings in their basal plane, they can adsorb on the graphite surface through $\pi-\pi$ interactions, which decreases the interfacial energy between the graphite and MeOH. Thus, the **GH25**, **GH50**, and **GH75** produced excellent dispersion of the graphite powder. However, **GH100** did not stabilize the graphite powder well because the large quantity of grafted hexylamine on **GH100** could prevent its interaction with the graphite. It was observed that 1 mg of **GH25**, **GH50**, and **GH75** dispersed 0.8, 1.8, and 3.0 mg of graphite, respectively, whereas **GH0** and **GH100** dispersed only 0.1 and 0.2 mg of graphite, respectively. It is also noted that the graphite dispersions using **GH25**, **GH50**, and **GH75** were highly stable for at least several months after the preparation (Figure 5b). In comparison, it is previously reported that the dispersion of graphite by GO was stable for a few days.[4] As shown in Figure 5c–e, the sizes of the dispersed graphite were decreased from 13.4 to 2.6 μm in the order of **GH25**, **GH50**, and **GH75**. In particular, **GH75** with well-balanced amphiphilicity exhibited excellent surfactant behavior in the oil–water system and was also the most effective dispersing agent for graphite.

CONCLUSIONS

We successfully synthesized a series of modified GQDs with tailored surface properties and demonstrated their use as efficient surfactants in immiscible blends. Wide-range control of the surface properties of the GQDs, from very hydrophilic to fully hydrophobic properties, was achieved in a systematic manner by grafting controlled amounts of the hexylamine onto the GQD surfaces. In addition, the reaction condition was very mild at 40 °C, so the reaction should not affect any of the intrinsic properties of the GQDs. The amphiphilic GQDs, i.e., **GH25**, **GH50**, and **GH75**, were located at the interface between two immiscible blends, and thus, the desired surfactant behavior was achieved with the modified GQDs. Specifically, these GQDs stabilized oil-in-water Pickering emulsions and the mini-emulsion polymerization of PS colloidal particles, the sizes

DOI: 10.1021/acsami.5b00729
ACS Appl. Mater. Interfaces 2015, 7, 8615–8621

of which were less than a few hundred nm. The GQDs were also used to control the dispersion of graphite in MeOH. Our strategy for controlling the surface activity of GQDs is a simple and versatile method that can extend the range of their application from emulsifiers to dispersing agents. More importantly, the synergistic combination of the fluorescence and surfactant properties of surface-modified GQDs can pave the way for promising applications, such as a fluorescent label and bioimaging.

■ ASSOCIATED CONTENT

Supporting Information

XPS, AFM, TEM, and additional data (PDF). This material is available free of charge via the Internet at http://pubs.acs.org.

■ AUTHOR INFORMATION

Corresponding Author

*E-mail: bumjoonkim@kaist.ac.kr.

Notes

The authors declare no competing financial interest.

■ ACKNOWLEDGMENTS

This research was supported by the Korea Research Foundation Grant funded by the Korean Government (2012R1A1A2A10041283).

■ REFERENCES

(1) Binks, B. P. Particles as Surfactants—Similarities and Differences. *Curr. Opin. Colloid Interface Sci.* **2002**, *7*, 21−41.

(2) Boker, A.; He, J.; Emrick, T.; Russell, T. P. Self-Assembly of Nanoparticles at Interfaces. *Soft Matter* **2007**, *3*, 1231−1248.

(3) Kwon, T.; Ku, K. H.; Kang, D. J.; Lee, W. B.; Kim, B. J. Aspect-Ratio Effect of Nanorod Compatibilizers in Conducting Polymer Blends. *ACS Macro Lett.* **2014**, *3*, 398−404.

(4) Kim, J.; Cote, L. J.; Kim, F.; Yuan, W.; Shull, K. R.; Huang, J. Graphene Oxide Sheets at Interfaces. *J. Am. Chem. Soc.* **2010**, *132*, 8180−8186.

(5) Jang, S. G.; Kim, B. J.; Hawker, C. J.; Kramer, E. J. Bicontinuous Block Copolymer Morphologies Produced by Interfacially Active, Thermally Stable Nanoparticles. *Macromolecules* **2011**, *44*, 9366−9373.

(6) Kim, B. J.; Fredrickson, G. H.; Hawker, C. J.; Kramer, E. J. Nanoparticle Surfactants as a Route to Bicontinuous Block Copolymer Morphologies. *Langmuir* **2007**, *23*, 7804−7809.

(7) Miesch, C.; Kosif, I.; Lee, E.; Kim, J.-K.; Russell, T. P.; Hayward, R. C.; Emrick, T. Nanoparticle-Stabilized Double Emulsions and Compressed Droplets. *Angew. Chem., Int. Ed.* **2012**, *51*, 145−149.

(8) Kang, D. J.; Kwon, T.; Kim, M. P.; Cho, C.-H.; Jung, H.; Bang, J.; Kim, B. J. Creating Opal-Templated Continuous Conducting Polymer Films with Ultralow Percolation Thresholds Using Thermally Stable Nanoparticles. *ACS Nano* **2011**, *5*, 9017−9027.

(9) Gubbels, F.; Jerome, R.; Teyssie, P.; Vanlathem, E.; Deltour, R.; Calderone, A.; Parente, V.; Bredas, J. L. Selective Localization of Carbon Black in Immiscible Polymer Blends: A Useful Tool To Design Electrical Conductive Composites. *Macromolecules* **1994**, *27*, 1972−1974.

(10) Elias, L.; Fenouillot, F.; Majeste, J. C.; Cassagnau, P. Morphology and Rheology of Immiscible Polymer Blends Filled with Silica Nanoparticles. *Polymer* **2007**, *48*, 6029−6040.

(11) Chen, T.; Colver, P. J.; Bon, S. A. F. Organic−Inorganic Hybrid Hollow Spheres Prepared from TiO_2-Stabilized Pickering Emulsion Polymerization. *Adv. Mater.* **2007**, *19*, 2286−2289.

(12) Li, L.; Miesch, C.; Sudeep, P. K.; Balazs, A. C.; Emrick, T.; Russell, T. P.; Hayward, R. C. Kinetically Trapped Co-continuous Polymer Morphologies through Intraphase Gelation of Nanoparticles. *Nano Lett.* **2011**, *11*, 1997−2003.

(13) Chung, H.-j.; Ohno, K.; Fukuda, T.; Composto, R. J. Self-Regulated Structures in Nanocomposites by Directed Nanoparticle Assembly. *Nano Lett.* **2005**, *5*, 1878−1882.

(14) Ku, K. H.; Yang, H.; Shin, J. M.; Kim, B. J. Aspect Ratio Effect of Nanorod Surfactants on the Shape and Internal Morphology of Block Copolymer Particles. *J. Polym. Sci., Part A: Polym. Chem.* **2015**, *53*, 188−192.

(15) Ku, K. H.; Shin, J. M.; Kim, M. P.; Lee, C.-H.; Seo, M.-K.; Yi, G.-R.; Jang, S. G.; Kim, B. J. Size-Controlled Nanoparticle-Guided Assembly of Block Copolymers for Convex Lens-Shaped Particles. *J. Am. Chem. Soc.* **2014**, *136*, 9982−9989.

(16) Hore, M. J. A.; Composto, R. J. Functional Polymer Nanocomposites Enhanced by Nanorods. *Macromolecules* **2013**, *47*, 875−887.

(17) Srivastava, S.; Schaefer, J. L.; Yang, Z.; Tu, Z.; Archer, L. A. 25th Anniversary Article: Polymer−Particle Composites: Phase Stability and Applications in Electrochemical Energy Storage. *Adv. Mater.* **2014**, *26*, 201−234.

(18) Melle, S.; Lask, M.; Fuller, G. G. Pickering Emulsions with Controllable Stability. *Langmuir* **2005**, *21*, 2158−2162.

(19) Madivala, B.; Vandebril, S.; Fransaer, J.; Vermant, J. Exploiting Particle Shape in Solid Stabilized Emulsions. *Soft Matter* **2009**, *5*, 1717−1727.

(20) Binks, B. P. Macroporous Silica From Solid-Stabilized Emulsion Templates. *Adv. Mater.* **2002**, *14*, 1824−1827.

(21) Kwon, T.; Kim, T.; Ali, F. b.; Kang, D. J.; Yoo, M.; Bang, J.; Lee, W.; Kim, B. J. Size-Controlled Polymer-Coated Nanoparticles as Efficient Compatibilizers for Polymer Blends. *Macromolecules* **2011**, *44*, 9852−9862.

(22) Hong, R. Y.; Fu, H. P.; Zhang, Y. J.; Liu, L.; Wang, J.; Li, H. Z.; Zheng, Y. Surface-Modified Silica Nanoparticles for Reinforcement of PMMA. *J. Appl. Polym. Sci.* **2007**, *105*, 2176−2184.

(23) Shenhar, R.; Norsten, T. B.; Rotello, V. M. Polymer-Mediated Nanoparticle Assembly: Structural Control and Applications. *Adv. Mater.* **2005**, *17*, 657−669.

(24) Daniel, M.-C.; Astruc, D. Gold Nanoparticles: Assembly, Supramolecular Chemistry, Quantum-Size-Related Properties, and Applications toward Biology, Catalysis, and Nanotechnology. *Chem. Rev.* **2003**, *104*, 293−346.

(25) Chung, H.-J.; Kim, J.; Ohno, K.; Composto, R. J. Controlling the Location of Nanoparticles in Polymer Blends by Tuning the Length and End Group of Polymer Brushes. *ACS Macro Lett.* **2011**, *1*, 252−256.

(26) Caruso, F. Nanoengineering of Particle Surfaces. *Adv. Mater.* **2001**, *13*, 11−22.

(27) Zhang, Z.; Zhang, J.; Chen, N.; Qu, L. Graphene Quantum Dots: an Emerging Material for Energy-Related Applications and Beyond. *Energy Environ. Sci.* **2012**, *5*, 8869−8890.

(28) Cheng, H.; Zhao, Y.; Fan, Y.; Xie, X.; Qu, L.; Shi, G. Graphene-Quantum-Dot Assembled Nanotubes: A New Platform for Efficient Raman Enhancement. *ACS Nano* **2012**, *6*, 2237−2244.

(29) Zhuo, S.; Shao, M.; Lee, S.-T. Upconversion and Down-conversion Fluorescent Graphene Quantum Dots: Ultrasonic Preparation and Photocatalysis. *ACS Nano* **2012**, *6*, 1059−1064.

(30) Zheng, X. T.; Than, A.; Ananthanaraya, A.; Kim, D.-H.; Chen, P. Graphene Quantum Dots as Universal Fluorophores and Their Use in Revealing Regulated Trafficking of Insulin Receptors in Adipocytes. *ACS Nano* **2013**, *7*, 6278−6286.

(31) Jin, S. H.; Kim, D. H.; Jun, G. H.; Hong, S. H.; Jeon, S. Tuning the Photoluminescence of Graphene Quantum Dots through the Charge Transfer Effect of Functional Groups. *ACS Nano* **2012**, *7*, 1239−1245.

(32) Li, Y.; Hu, Y.; Zhao, Y.; Shi, G.; Deng, L.; Hou, Y.; Qu, L. An Electrochemical Avenue to Green-Luminescent Graphene Quantum Dots as Potential Electron-Acceptors for Photovoltaics. *Adv. Mater.* **2011**, *23*, 776−780.

(33) Pan, D.; Zhang, J.; Li, Z.; Wu, M. Hydrothermal Route for Cutting Graphene Sheets into Blue-Luminescent Graphene Quantum Dots. *Adv. Mater.* **2010**, *22*, 734−738.

DOI: 10.1021/acsami.5b00729
ACS Appl. Mater. Interfaces 2015, 7, 8615−8621

(34) Guo, C. X.; Dong, Y.; Yang, H. B.; Li, C. M. Graphene Quantum Dots as a Green Sensitizer to Functionalize ZnO Nanowire Arrays on F-Doped SnO2 Glass for Enhanced Photoelectrochemical Water Splitting. *Adv. Energy Mater.* **2013**, *3*, 997−1003.
(35) Zhu, Y.; Murali, S.; Cai, W.; Li, X.; Suk, J. W.; Potts, J. R.; Ruoff, R. S. Graphene and Graphene Oxide: Synthesis, Properties, and Applications. *Adv. Mater.* **2010**, *22*, 3906−3924.
(36) Dreyer, D. R.; Park, S.; Bielawski, C. W.; Ruoff, R. S. The Chemistry of Graphene Oxide. *Chem. Soc. Rev.* **2010**, *39*, 228−240.
(37) Zhu, S.; Zhang, J.; Tang, S.; Qiao, C.; Wang, L.; Wang, H.; Liu, X.; Li, B.; Li, Y.; Yu, W.; Wang, X.; Sun, H.; Yang, B. Surface Chemistry Routes to Modulate the Photoluminescence of Graphene Quantum Dots: From Fluorescence Mechanism to Up-Conversion Bioimaging Applications. *Adv. Funct. Mater.* **2012**, *22*, 4732−4740.
(38) Tetsuka, H.; Asahi, R.; Nagoya, A.; Okamoto, K.; Tajima, I.; Ohta, R.; Okamoto, A. Optically Tunable Amino-Functionalized Graphene Quantum Dots. *Adv. Mater.* **2012**, *24*, 5333−5338.
(39) Qian, Z.; Ma, J.; Shan, X.; Shao, L.; Zhou, J.; Chen, J.; Feng, H. Surface Functionalization of Graphene Quantum Dots with Small Organic Molecules from Photoluminescence Modulation to Bioimaging Applications: an Experimental and Theoretical Investigation. *RSC Adv.* **2013**, *3*, 14571−14579.
(40) Peng, J.; Gao, W.; Gupta, B. K.; Liu, Z.; Romero-Aburto, R.; Ge, L.; Song, L.; Alemany, L. B.; Zhan, X.; Gao, G.; Vithayathil, S. A.; Kaipparettu, B. A.; Marti, A. A.; Hayashi, T.; Zhu, J.-J.; Ajayan, P. M. Graphene Quantum Dots Derived from Carbon Fibers. *Nano Lett.* **2012**, *12*, 844−849.
(41) Yang, H.; Kang, D. J.; Ku, K. H.; Cho, H.-H.; Park, C. H.; Lee, J.; Lee, D. C.; Ajayan, P. M.; Kim, B. J. Highly Luminescent Polymer Particles Driven by Thermally Reduced Graphene Quantum Dot Surfactants. *ACS Macro Lett.* **2014**, 985−990.
(42) Razmi, H.; Mohammad-Rezaei, R. Graphene Quantum Dots as a New Substrate for Immobilization and Direct Electrochemistry of Glucose Oxidase: Application to Sensitive Glucose Determination. *Biosens. Bioelectron.* **2013**, *41*, 498−504.
(43) Kim, F.; Cote, L. J.; Huang, J. Graphene Oxide: Surface Activity and Two-Dimensional Assembly. *Adv. Mater.* **2010**, *22*, 1954−1958.
(44) Dong, Y.; Chen, C.; Zheng, X.; Gao, L.; Cui, Z.; Yang, H.; Guo, C.; Chi, Y.; Li, C. M. One-step and High Yield Simultaneous Preparation of Single- and Multi-Layer Graphene Quantum Dots from CX-72 Carbon Black. *J. Mater. Chem.* **2012**, *22*, 8764−8766.
(45) Zhu, S.; Zhang, J.; Qiao, C.; Tang, S.; Li, Y.; Yuan, W.; Li, B.; Tian, L.; Liu, F.; Hu, R.; Gao, H.; Wei, H.; Zhang, H.; Sun, H.; Yang, B. Strongly Green-Photoluminescent Graphene Quantum Dots for Bioimaging Applications. *Chem. Commun.* **2011**, *47*, 6858−6860.
(46) Aveyard, R.; Binks, B. P.; Clint, J. H. Emulsions Stabilised Solely by Colloidal Particles. *Adv. Colloid Interface Sci.* **2003**, *100−102*, 503−546.
(47) Vignati, E.; Piazza, R.; Lockhart, T. P. Pickering Emulsions: Interfacial Tension, Colloidal Layer Morphology, and Trapped-Particle Motion. *Langmuir* **2003**, *19*, 6650−6656.
(48) Sun, Z.; Feng, T.; Russell, T. P. Assembly of Graphene Oxide at Water/Oil Interfaces: Tessellated Nanotiles. *Langmuir* **2013**, *29*, 13407−13413.
(49) He, Y.; Wu, F.; Sun, X.; Li, R.; Guo, Y.; Li, C.; Zhang, L.; Xing, F.; Wang, W.; Gao, J. Factors that Affect Pickering Emulsions Stabilized by Graphene Oxide. *ACS Appl. Mater. Interfaces* **2013**, *5*, 4843−4855.
(50) Thickett, S. C.; Zetterlund, P. B. Preparation of Composite Materials by Using Graphene Oxide as a Surfactant in Ab Initio Emulsion Polymerization Systems. *ACS Macro Lett.* **2013**, *2*, 630−634.
(51) Che Man, S. H.; Thickett, S. C.; Whittaker, M. R.; Zetterlund, P. B. Synthesis of Polystyrene Nanoparticles "Armoured" with Nano-dimensional Graphene Oxide Sheets by Miniemulsion Polymerization. *J. Polym. Sci., Part A: Polym. Chem.* **2013**, *51*, 47−58.
(52) Sandeep Kumar, G.; Roy, R.; Sen, D.; Ghorai, U. K.; Thapa, R.; Mazumder, N.; Saha, S.; Chattopadhyay, K. K. Amino-functionalized graphene quantum dots: origin of tunable heterogeneous photo-luminescence. *Nanoscale* **2014**, *6*, 3384−3391.

DOI: 10.1021/acsami.5b00729
ACS Appl. Mater. Interfaces 2015, 7, 8615−8621